

# DTIC FILE COPY

2

SECURITY CLASSIFICATION OF THIS PAGE

## REPORT DOCUMENTATION PAGE

Form Approved  
OMB No. 0704-0188

1a. REPORT SECURITY CLASSIFICATION  
**UNCLASSIFIED**

**DTIC**

1b. RESTRICTIVE MARKINGS

2a. SECURITY CLASSIFICATION AUTHORITY

**ELECTE**  
**EP 27 1990**

3. DISTRIBUTION/AVAILABILITY OF REPORT

Approved for public release;  
distribution is unlimited

# AD-A226 792

IR(S)

5. MONITORING ORGANIZATION REPORT NUMBER(S)

AFOSR-TR- 00 1040

6b. OFFICE SYMBOL  
(if applicable)

7a. NAME OF MONITORING ORGANIZATION

AFOSR/NA

University of Toronto

6c. ADDRESS (City, State, and ZIP Code)

200 College St.  
Toronto, Ontario M5S 1A4

7b. ADDRESS (City, State, and ZIP Code)

Building 410, Bolling AFB DC  
20332-6448

8a. NAME OF FUNDING/SPONSORING ORGANIZATION  
AFOSR

8b. OFFICE SYMBOL  
(if applicable)  
NA

9. PROCUREMENT INSTRUMENT IDENTIFICATION NUMBER

AFOSR-89-0365

8c. ADDRESS (City, State, and ZIP Code)

Building 410, Bolling AFB DC  
20332-6448

10. SOURCE OF FUNDING NUMBERS

PROGRAM ELEMENT NO.	PROJECT NO.	TASK NO.	WORK UNIT ACCESSION NO.
61102F	2302	B1	-

11. TITLE (Include Security Classification)

Mesomechanical Model for Fibre Composites (U)

12. PERSONAL AUTHOR(S)

Piggott, Michael R.

13a. TYPE OF REPORT  
Annual Progress

13b. TIME COVERED  
FROM 89/6/1 TO 90/5/31

14. DATE OF REPORT (Year, Month, Day)  
90/07/30

15. PAGE COUNT  
19

16. SUPPLEMENTARY NOTATION

17. COSATI CODES

FIELD	GROUP	SUB-GROUP
	20.11	

18. SUBJECT TERMS (Continue on reverse if necessary and identify by block number)

Fibre Reinforced Polymers, Mechanics of Composites. (15)

19. ABSTRACT (Continue on reverse if necessary and identify by block number)

Experimental work has proceeded according to schedule in two areas: debonding of interfaces and the production and testing of short aligned fibre composites. In addition some theoretical work has been carried out.

**Interfaces.** Carbon fibre interfaces with epoxy resins have been examined using the fibre pull out method. This method can now be reliably and reproducibly used to measure the bond strength. Shear strengths can be very high, up to nearly 150 MPa in individual experiments, with average values for 50 or more tests of up to 100 MPa. The strengths are little different for Hercules AS1, AS2 and AS4. The sizing appears to have little effect (but this needs to be confirmed). The strengths observed are up to three times the shear strength of the polymer. Carbon and glass interfaces with thermoplastics (polyethylene and nylon) can also be measured using this method. Results here are up to four times the estimated shear strength of the polymer. To explain the high results an equivalent work of fracture is involved. This has never exceeded 300 Jm<sup>-2</sup>, indicating that the interphases are quite brittle. (continue on reverse side)

20. DISTRIBUTION/AVAILABILITY OF ABSTRACT  
 UNCLASSIFIED/UNLIMITED  SAME AS RPT.  DTIC USERS

21. ABSTRACT SECURITY CLASSIFICATION  
UNCLASSIFIED

22a. NAME OF RESPONSIBLE INDIVIDUAL  
G. Hariton

22b. TELEPHONE (Include Area Code)  
(202) 767-0463

22c. OFFICE SYMBOL  
AFOSR/NA



**MESOMECHANICAL MODEL FOR FIBRE COMPOSITES:  
THE ROLE OF THE INTERFACE**

**M.R. Piggott**

**Department of Chemical Engineering & Applied Chemistry  
University of Toronto, Toronto, Ontario M5S 1A4  
Canada**

**EXECUTIVE SUMMARY**

Experimental work has proceeded according to schedule in two areas: debonding of interfaces and the production and testing of short aligned fibre composites. In addition some theoretical work has been carried out.

**Interfaces**

Carbon fibre interfaces with epoxy resins have been examined using the fibre pull out method. This method can now be reliably and reproducibly used to measure the bond strength. Shear strengths can be very high, up to nearly 150 MPa in individual experiments, with average values for 50 or more tests of up to 100 MPa. The strengths are little different for Hercules AS1, AS2 and AS4. The sizing appears to have little effect (but this needs to be confirmed). The strengths observed are up to three times the shear strength of the polymer. Carbon and glass interfaces with thermoplastics (polyethylene and nylon) can also be measured using this method. Results here are up to four times the estimated shear strength of the polymer. To explain the high results an equivalent work of fracture is involved. This has never exceeded  $300 \text{ Jm}^{-2}$ , indicating that the interphases are quite brittle.

**Short Fibre Composites**

Aligned fibre composites have been made with 2 mm long carbon fibres. Their strengths and Young's moduli were somewhat less than expected. It seems highly probable that this is due

to imperfection in the structures produced. Some indication of this comes from off-axis tests, but further work is needed to determine the precise structure.

### **Theoretical Developments**

Mesomechanics has already played a role in improving the understanding of compression and fatigue properties of aligned fibre composites. What is particularly important for the development of this branch of mechanics is the identification and precise characterization of the structure in a real composite. This involves mesostructures, hitherto mostly unrecognized. Mesostructures are herein defined as intermediate between the micro and macrostructures, and usually fortuitous. Examples are fibre bundling, fibre waviness, and end synchronization. They are classified as Adventitious Disorder and Adventitious Order effects, and subclassified as orientation and packing errors. It is expected that this concept will be very helpful in explaining results obtained with short fibres composites as well as compression and fatigue.

### **1. INTRODUCTION**

Mesomechanics adopts a heterogeneous approach to the prediction of mechanical properties of fibre composites (and other materials) rather than the continuum mechanics adopted heretofore [1]. A major challenge is to describe the complex substructures involved in ways that may be used to develop governing equations for global properties. Another challenge is to include the kinematics of microstructural evolution, i.e. the development of damage during use.

During the relatively short history of synthetic fibre composites, governing equations for mechanical properties have been developed for fibre-interface-polymer microstructures which translate into global properties. These show that simple mixture rules, or modifications thereof such as the Tsai-Halpin equations [2], can predict elastic properties of continuous fibre composites. However, they are not so successful with short fibre composites [3].

In addition, it has been found that simple micromechanical theories do not adequately predict strengths. This is particularly noticeable in the case of the compressive strength of the composite [4].

The program of research described here is an attempt to bridge the micromechanics-continuum mechanics gap. It involves both an experimental program and a theoretical approach. These will be described in turn.

## **2. EXPERIMENTS ON THE FIBRE-MATRIX INTERFACE**

The single fibre pull out experiment has been adopted for this, since it permits the measurement of debonding force as a function of embedded length. This enables some conclusions to be drawn about the nature of the interface failure mechanism, as well as giving values for debonding stress and in some cases interfacial pressure and friction as well.

### **2.1 Experimental Method**

A special set up has been designed and developed for the embedding of fibres, fig. 1. This is a carousel arrangement, which is used for embedding 39 fibres in one operation. Good geometry of embedment is assured by holding the fibres vertically in glass capillaries fixed inside brass tubes which can slide up and down in the upper section of the carousel. The embedment length is controlled by using a micrometer mechanism to lower the tube containing the fibre, meanwhile observing the fibre end and the resin container through a microscope.

When 39 fibres have been placed to the correct depths in the liquid resin, the whole carousel assembly is put in the oven for cure.

The process has been adapted, for use with low melting temperature thermoplastics, by mounting the carousel on a heater. The polymer is melted, and the fibres are then lowered into small depressions made in the polymer surface. (Equipment to be used for higher melting temperature thermoplastics is still under development.)

After embedment, and cure where necessary, the fibres are removed from the carousel and tested in an Instron machine. Here, special precautions are taken to ensure that the fibre stress is axial. A plate is held in the upper grip of the machine, and the fibre brought into contact with it, and then bonded to it with cyanoacrylate adhesive. Pull out is carried out at  $0.5 \text{ mm min.}^{-1}$ .

## **2.2. Experimental Results**

### **2.2.1 Thermosets**

Tests have been carried out with Hercules carbon fibres AS1 (unsized), AS2 (sized), AS4 (sized) and HMU in Shell epoxy resins EPON 815 and 828. For the EPON 815 the curing agent was Anchor 1170, and the curing was at temperatures in the range 60-180°C. For the EPON 828, Anchor 1115 was used, and the resin was cured at 135°C for 22 hr.

Fig. 2 shows two typical pull out curves. Here the force is plotted as a function of distance pulled out. With a well adhering fibre, labelled AS4, the force increases linearly until debonding occurs. At this instant the force falls precipitately, and the remainder of the pull out is governed by friction. With a poorly adhering fibre, labelled HMU, debonding and friction immediately thereafter involve almost the same force, and the force is much smaller than in the well bonded case.

Figs. 3-6 show the debonding forces ( $F_A$ ) as a function of embedded length  $L$  for AS1 in EPON 815 with different amounts of curing.  $F_A$  is proportional to  $L$  up to about 0.10 to 0.15 mm. Thereafter it has a plateau region at a level of about 0.2N. The lower embedded length region corresponds to an approximately constant debonding stress which may possibly increase with increasing degree of cure: 100°C, 0.5 h gives 56 MPa, 60°C, 4 h gives 59 MPa, 180°C, 0.5 gives 61 MPa and 180°C, 4 h gives 73 MPa. These results however, involve coefficients of variation of 12-25% (see table 1).

HMU hardly bonds at all to epoxy resin; the frictional part of the pull out curve, see Fig. 2, gives about the same shear stress as the debonding part. This should be contrasted with the pull out curve for AS4 in the same resin (EPON 828), with the same cure, i.e. 22 h at 135°C, where the debonding force greatly exceeds the frictional force. Fig. 7 shows that  $F_A$  is approximately proportional to  $L$ , corresponding to a shear stress of about 2.9 MPa when the debonding force is greater than the initial frictional force. A similar conclusion emerges from results where the debonding force is less than the frictional force, fig. 8.

AS1, AS2, and AS4 all give about the same results when embedded in EPON 828 cured at 135°C for 22 h. figs. 9-11 and table 1. The mean and maximum debonding stresses are extremely high, i.e. up to nearly 150 MPa for the maximum and 100 MPa for the mean.

### **2.2.2 Thermoplastics**

With nylon and polyethylene, the pull out curve shows some evidence of plastic yielding, see fig. 12. With AS4 fibres the debonding stress for polyethylene (fig. 13) is much less than for epoxy (fig. 11). There is some indication of a plateau for  $L > 0.8$  mm. The average debonding stress is about 12 MPa.

With glass fibres, figs. 14-16, the results are very similar. All the results with thermoplastics are highly scattered.

### **2.3 Interpretation of Results**

The interface or interphase, in the case of the epoxy, appears to be extremely strong. Tests on the EPON 815 indicate a compressive yield stress in the range 45-60 MPa, with an ultimate compressive strength of 80-90 MPa. Curing at 60°C for 4 h gives much the same result as 180°C for 4 h. Thus polymer adjacent to the interphase is expected to yield in shear at 26-35 MPa (Von Mises yield criterion). The mean interface stresses observed with EPON 815 (table 1) are 56-73 MPa with maxima as high as 100 MPa. Thus ductile failure at the interface is highly improbable with surface treated AS1 in EPON 815. This is also the case with AS1 and AS2 and AS4 in EPON 828, where the interphase strength is even greater.

The debonding stress,  $\tau_d$  is associated with an equivalent work of fracture in the interphase,  $G_i$ , [5], where

$$G_i = d\tau_d^2(1+\nu_m)\ln(D/d)/2E_m \quad (1)$$

Here  $d$  is the fibre diameter, and  $D$  is the diameter of the cylinder of resin in which it had been embedded.  $\nu_m$  and  $E_m$  are the Poisson's ratio and Young's modulus of the polymer. Values of  $G_i$  associated with the debonding stresses are given in table 1. These values are all less than  $300 \text{ Jm}^{-2}$ , indicating that the interphase could possibly fail quite easily by brittle fracture.

The effect of fibre type is not apparently very great, at least as between AS1, AS2 and AS4, and the sizing appears to make very little difference. This needs to be confirmed however, as a comparison between sized and unsized fibres with the same type of polymer has not yet been made. The beneficial effects of surface treatment are very evident however, with the low result from the HMU.

With low temperature thermoplastics the interphase is evidently much weaker. Again, however, it is stronger than the shear strength of the polymer,  $\tau_{mu}$ . For the polyethylene, this was about 3 MPa, so the mean debonding stresses were about 400% greater in this case. Again, there are very low equivalent works of fracture (table 1) which indicate easy failure by brittle fracture.

### **3. SHORT FIBRE COMPOSITES**

#### **3.1. Experimental Method**

A specially constructed machine [3] was used to produce aligned fibre mats. This involved dispersing the fibres in glycerine, and spreading them on the inside of a rotating cylindrical screen, fig. 17. (The rotation removed the glycerine.) Alignment was obtained with 2 mm long fibres when a 2 mm diameter converging nozzle was used, and set 8-10 mm above the mesh. The drum rotated at 400 rpm and the nozzle traversed the drum at  $17 \text{ mm s}^{-1}$ . Hercules AS2-W-12k fibres were used. The fibre angular distribution is shown in fig. 18.

Composites were made using EPON 828 with 7.0% Anchor 1115. For this, several layers of cleaned and dried mat were placed in a mold, infiltrated with the resin mixture, and then hot pressed at a pressure of no more than 3 MPa and  $135^\circ\text{C}$ . The final thickness of the composite was 1.5 mm for tensile and flexure tests and 3 mm for Izod tests.

For tensile testing, 20 mm x 50 mm end tabs were bonded to the specimen using epoxy. They were tested in an MTS machine at 0.5 mm min<sup>-1</sup>. Flexure tests were carried out at the same rate, using 4 point bending with a gauge length of 25.4 mm and a lever arm length of 12.7 mm. Rollers were used at the loading points. For the Izod tests a Tinius Olsen Impact Tester was used.

### **3.2 Experimental Results**

The tensile strengths of the 2 mm long aligned fibre composites so far produced do not fit a linear relationship with fibre volume fraction,  $V_f$ , very well, see fig. 19. Also shown on the figure is the expected strength of continuous aligned fibre composites,  $\sigma_{1uR}$ , given by the expression

$$\sigma_{1uR} = V_f \sigma_{fu} + V_m E_m \sigma_{fu} / E_f \quad (2)$$

(Here  $\sigma_{fu}$  is the fibre strength,  $E_f$  its Young's modulus,  $E_m$  is the modulus of the polymer and  $V_m$  its volume fraction.) Flexural strengths were somewhat higher, fig. 20, but at the higher volume fractions there was a fall off in strength. When the composites were strained in tension prior to testing in bending their flexural strengths were reduced.

The Young's moduli of the composites were about 80% of the Rule of Mixtures values, see. fig. 21, at least up to  $V_f = 0.25$ . Thereafter the rate of increase in modulus with increasing  $V_f$  was less. The work of fracture of the composites was a linear function of  $V_f$ , fig. 22, but with an intercept at  $V_f \cong 0.13$ .

Off-axis tests showed a drop off in properties with angle between the fibres and the tensile stress. Fig. 22 shows the strength with the line labelled theory estimated using the Tsai-Hill equations. Fig. 23 shows the Young's modulus with the theoretical line estimated from the standard expression containing  $\cos^4\theta$  etc. In both cases the drop off with  $\theta$  was less than expected.

### **3.3 Interpretation of Results**

The critical length of the fibres,  $l_c$ , from the pull out work was about 0.2 mm, i.e. about one tenth of the fibre length,  $l$ . Since, in theory at least, the composite strength,  $\sigma_{1u}$  is given by

$$\sigma_{1u} = V_f(1-l_c/2l)\sigma_{fu} + V_m E_m \sigma_{fu} / E_f \quad (3)$$

we should expect only a 5% loss in strength due to the short fibre length. Imperfect alignment could possibly cause some additional loss. Using the modulus results, to estimate the effect of this as about 20% loss, we would expect about 25% loss overall. The flexural test results, at least up to  $V_f = 0.27$ , give about 32% loss. This suggests that some other factors are affecting the results.

The tensile strengths were somewhat low. Since they were much less than the flexural strengths it seems highly probable that we have a problem with our testing technique. These short fibre composites appear to be more difficult to grip than regular aligned continuous fibre laminates. Future efforts will be directed towards solving this problem.

For  $V_f > 0.3$  the properties fall off. This was observed in previous work [3] and could be due to excessive voids (~3%). Effort will therefore be directed towards reducing void content. Prestraining the composite also leads to some loss in strength. Further work will be directed towards elucidating the mechanisms contributing to this.

The off-axis results are probably due to imperfect alignment. Further work will be done on this also.

## **4. THEORETICAL DEVELOPMENTS**

The key to the development of mesomechanics may well lie in a better understanding of the substructures involved. Heretofore it has been almost universally assumed that a two step approach could be used: i.e. 1) from micromechanics directly to lamina and then 2) from lamina to laminate properties. That this is probably erroneous is apparent when we look at compressive strength

prediction. Efforts to do this on the basis of the simple micromechanical approach [6] have been unsuccessful [4]. Instead, a major contribution to compressive failure comes from lack of perfect fibre alignment, and there is a direct correlation between fibre alignment and strength and modulus in compression [7]. However, prediction of compressive strength may also require inclusion of fibre bundle effects [4].

Fibre waviness and fibre bundles constitute substructures which are not normally intended to be present in a composite. We will call such substructures mesostructures.

#### **4.1 Mesostructures**

Mesostructures will be defined here as structures which are coarser than the fibre-interface-polymer microstructure, but on a finer scale than the lay-up, core-skin structure and outer form of the material. They are generally a fortuitous structure, i.e. not part of the original design.

At least two classes of mesostructure can be identified, since we can have disorder in what is intended to be a rigidly ordered structure, and conversely, order in what is intended to be a disordered structure. Within each class there are at least two types of order/disorder: orientation effects and packing effects. We will discuss the two classes separately.

#### **4.2 Adventitious Disorder**

##### **4.2.1 Orientation Errors**

Even in the best laid up laminates it is impossible to ensure that the fibres are perfectly straight, yet perfect straightness is assumed in practically all theoretical treatments of fibre composites. This lack of straightness shows up as imperfect alignment or a fibre waviness. This will directly affect the compression strength (and modulus), shear strength, delamination resistance, and fatigue endurance (including tension-tension fatigue). There may also be secondary effects on tensile modulus and strength, and fracture toughness. Local misorientations can be quantified using the method of Yurgartis [8] but fibre waviness is more difficult to measure.

### **4.2.2 Packing Faults**

Normally, theoretical treatments assume hexagonal packing of fibres in three dimensional aligned fibre structures, although square packing is sometimes assumed. Laminates are treated theoretically as though, in each lamina, there is a single layer of fibres, equispaced, and with axes located on the centre plane of the lamina. Real composites, on the other hand, contain resin rich areas which are relatively weak, and resin poor areas where contacts can occur. The most serious example of packing faults, moreover, is the lack of either fibre or resin in some regions, i.e. voids in the structure. All composites appear to contain voids.

The main effect of these faults will be to reduce the various strengths of a composite: tensile, compression, shear etc. However, if the composite contains excessive voids (a good composite has roughly one volume per cent of them) the moduli could also be affected.

## **4.3 Adventitious Order**

### **4.3.1 Orientation Effects**

In a random mat or a sheet molding compound, the orientation of the fibres is seldom completely random, although normally complete randomness is usually intended. The process of molding these materials can also develop preferred orientations. These will give the composite unexpectedly high properties in some directions, and correspondingly low properties in others. Similar effects are observed when short fibre reinforced thermoplastics (e.g. nylon) are molded. The orientation of the fibres inside the molding is complex, and reflects the flow pattern. For example, in thin sections the fibres are usually preferentially oriented parallel to the plane of the mold surfaces. Design data for such moldings must take these mesostructures into account.

### **4.3.2 Packing Effects**

In short fibre composites, the fibre ends are expected to be positioned at random. However, imperfect dispersion can result in some end synchronization, i.e. fibre ends may be concentrated in (or close to) particular planes. This will weaken the composite. In continuous and

in long fibre composites fibre bundling can occur. In this case fibre bundles (perhaps from the original roving or tow; especially if it sustains a little twist) retain their presence in the composite, and act in harmony. This can increase the across-the-grain toughness of a composite, and reduces the compressive strength.

#### **4.4 Prediction of Properties Using Mesomechanics**

This already appears to be possible in the case of compression strength, and some progress has been made in fatigue of carbon fibre composites [9]. Further developments will require a much greater attention to details of the mesostructure.

In the case of the short fibre composites studied here we need to examine orientation errors, packing faults (especially voids) and fibre end synchronization. The first step here will be an attempt to quantify them.

### **5. MILESTONES ACHIEVED**

**Milestone #1** Materials have been assembled and fibres have been cut. The initial fibre cutting was not successful, and a different company has cut some more fibres. However, we still need HMS fibres cut. This is on hand. Short fibre composites have been made, and procedures established.

**Milestone #2** Debonding forces as a function of length have been measured with high breaking strain fibres, and short aligned fibre composites made. Strength and moduli have been measured, and overall quality including void content and fibre alignment has been assessed.

Further work is still needed on void content and quality assessment, but we are ahead of schedule in having done flexure tests, prestraining tests and off-axis tests.

## **6. CONCLUSIONS**

1. Fibre-polymer interphase strengths can be reliably measured using the fibre pull out test. The strengths estimated from these tests were extremely high, i.e. up to four times the estimated shear strength of the polymer. However, if failure is governed by brittle fracture, the work of fracture is quite low, i.e. less than  $300 \text{ Jm}^{-2}$  in the cases examined.

2. Fibre mats with reasonably well aligned carbon fibres can be produced, and reinforced epoxy composites made from them. The mechanical properties of these composites are lower than expected. There is a possibility that the precise structure being produced is an important factor here.

3. Mesomechanics appears likely to be highly important for the understanding of composite properties. What is particularly significant in the translation of micro to macromechanics is the precise structure. A number of different mesostructures have been recognized and classified as order/disorder effects associated with orientation and packing.

4. The work is up to schedule according to the original plan.

## **REFERENCES**

1. G.K. Haritos, J.W. Hager, A.K. Amos and M.J. Salkind, *Int. J. Solids Structures* **24**, (1988), 1081.
2. J.E. Ashton, J.C. Halpin and P.H. Petit, "Primer on Composite Materials: Analysis", (Technomic, Westport, Conn. 1969)
3. A.R. Sanadi and M.R. Piggott, *J. Mater. Sci.* **20**, (1985), 421.
4. M.R. Piggott, *J. Mater. Sci.* **16**, (1981), 2837.
5. M.R. Piggott, *Composite Science & Technology*, submitted (1990).
6. B.W. Rosen, "Composite Materials", (American Soc. for Metals, Ohio, 1964), Chpt. 3.
7. A. Mrse and M.R. Piggott, 36th SAMPE Symp. (1990), 2236.
8. S.W. Yurgartis, *Comp. Sci. Tech.* **30**, (1987), 279.
9. M.R. Piggott and P.W.K. Lam, ASTM STP, accepted for publication (1989).

**TABLE 1.**  
**DEBONDING DATA FROM PULL OUT EXPERIMENTS**

<b>Fibre</b>	<b>Resin</b>	<b>Cure Temp. (°C)</b>	<b>Time (h)</b>	<b>Debonding Stress (MPa)</b> <b>Maximum</b>	<b>Mean</b>	<b>Work of Fracture (Jm<sup>-2</sup>)</b>
AS1*	815	100	0.5	76	56 ± 71	38
AS1*	815	180	0.5	83	61 ± 11	45
AS1*	815	60	4	72	59 ± 11	42
AS1*	815	180	4	100	73 ± 18	64
HMU	828	135	22	8	2.9 ± 1.3	
HMU+	828	135	22	2.3	1.7 ± 0.3	
AS1	828	135	22	146	100 ± 19	120
AS2	828	135	22	139	84 ± 24	85
AS4	828	135	22	119	88 ± 11	93
AS4	LDPE			28	12 ± 5	16
Glass	LDPE			29	13 ± 4	18
Glass*	LDPE			13	12 ± 1	16
Glass	Nylon 12			49	18 ± 10	10

\* Unsized fibres  
+ Frictional Results

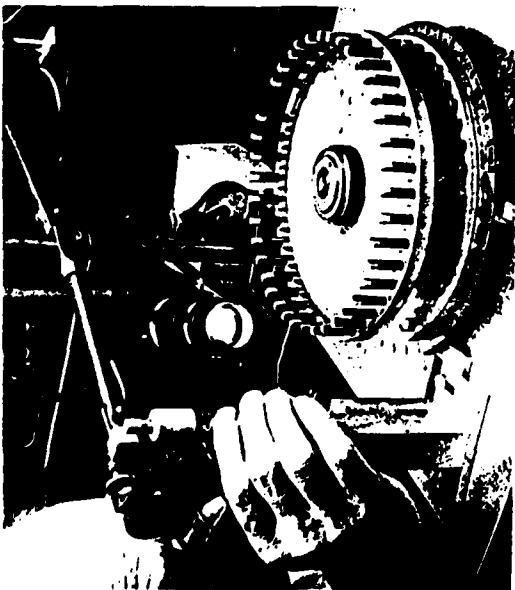


Fig. 1. Experimental set up used for embedding fibres prior to pull out experiment.

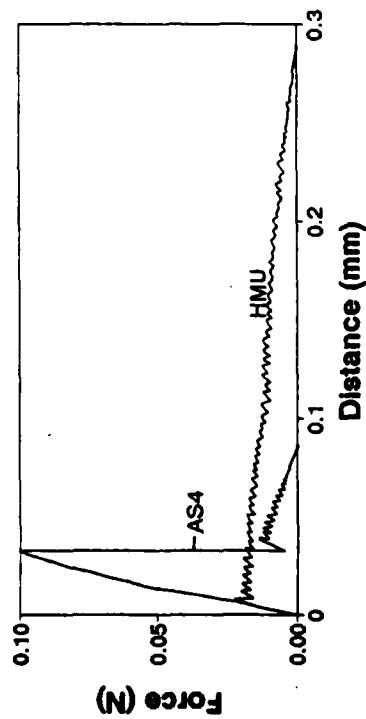


Fig. 2. Force vs distance moved during pull out. HMU and AS4 fibres embedded in EPON 828.

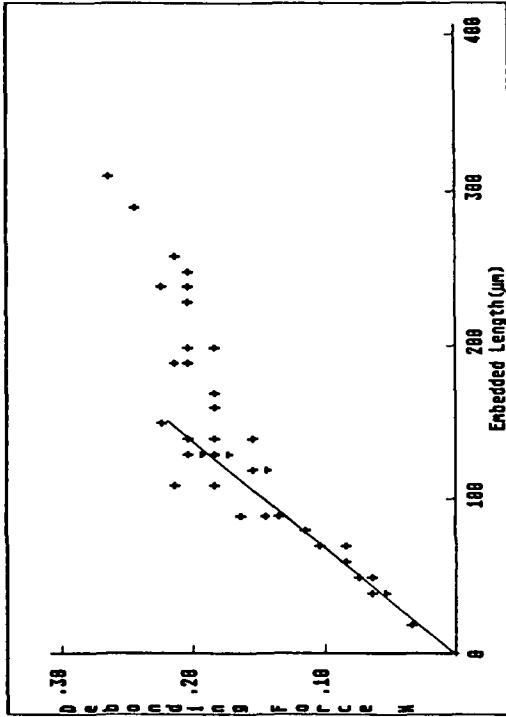


Fig. 3. Debonding force vs embedded length. AS1 fibres in EPON 815 cured at 100°C for 1/2 h.

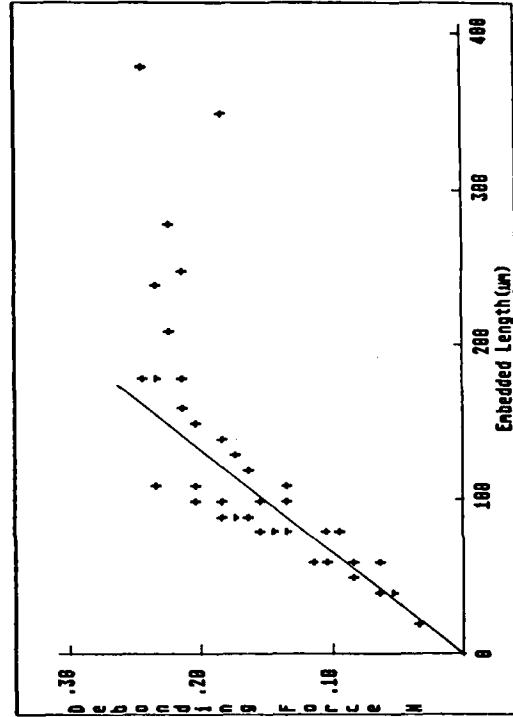


Fig. 4. Debonding force vs embedded length. AS1 fibres in EPON 815 cured at 180°C for 1/2 h.

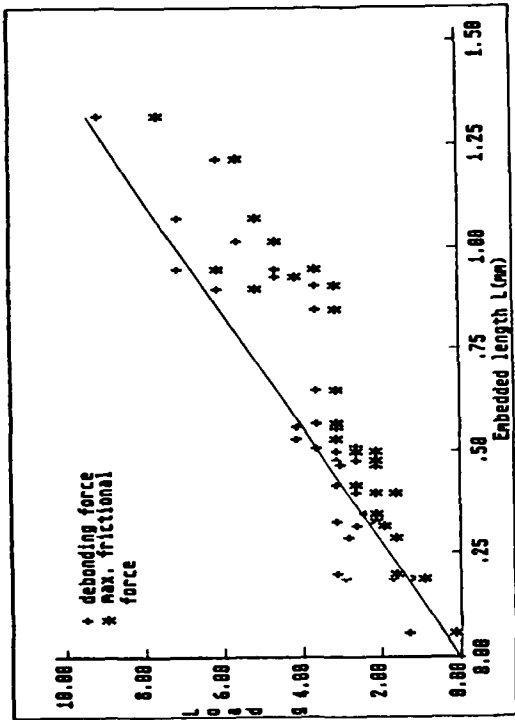


Fig. 7. Debonding force vs embedded length. HMU in EPON 828 cured at 135°C for 22 h.

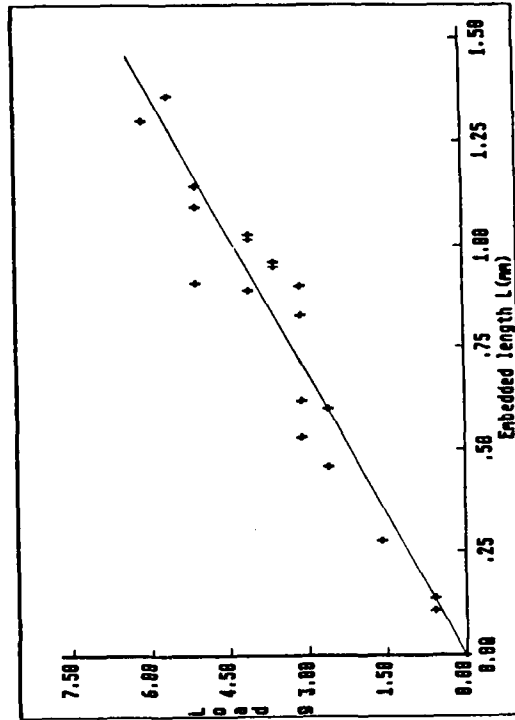


Fig. 8. Debonding force vs embedded length. HMU in EPON 828 cured at 135°C for 22 h. Results for debonding force when less than friction force.

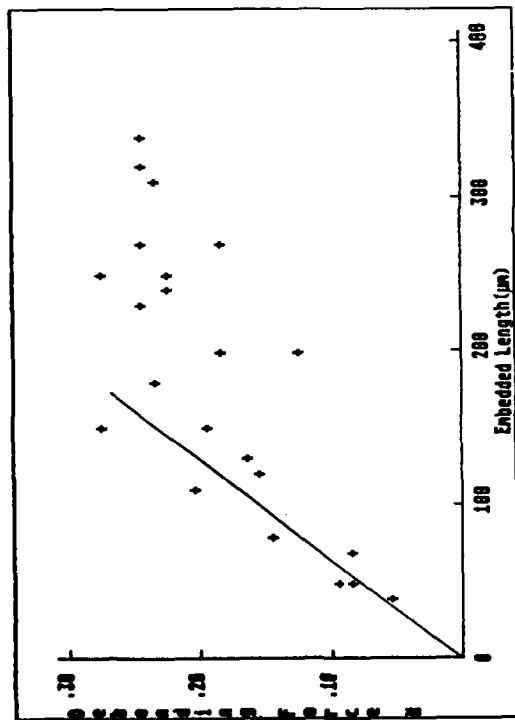


Fig. 5. Debonding force vs embedded length. AS1 fibres in EPON 815 cured at 60°C for 4 h.

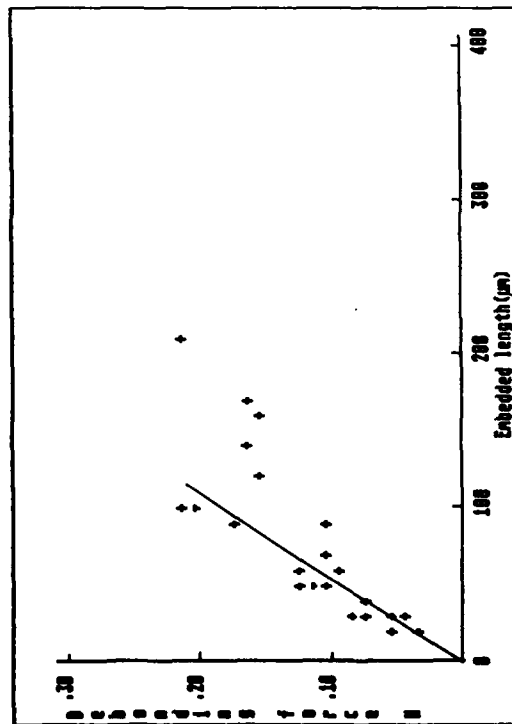


Fig. 6. Debonding force vs embedded length. AS1 fibres in EPON 815 cured at 180°C for 4 h.

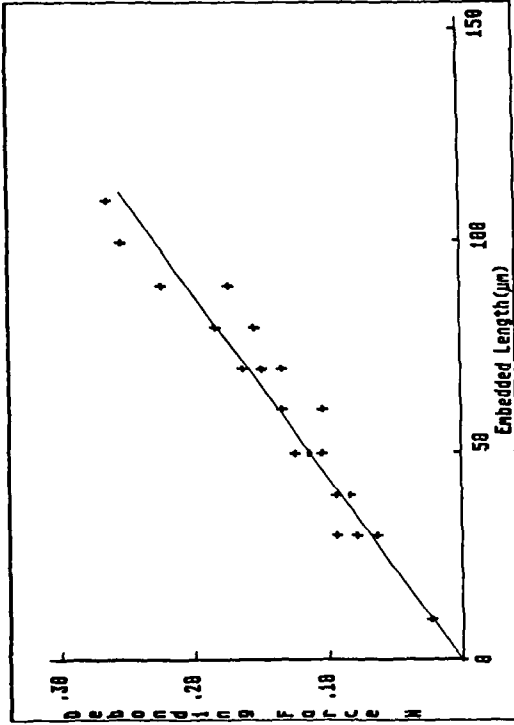


Fig. 11. Debonding force vs embedded length. AS4 fibres in EPON 815 cured at 60°C for 4 h.

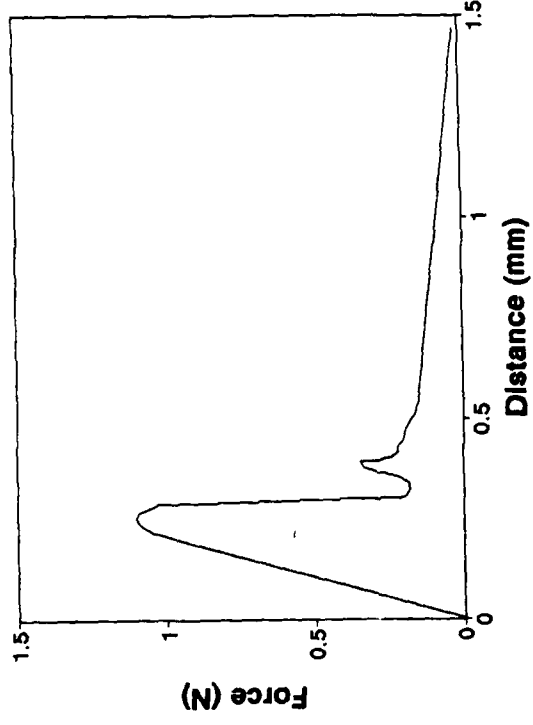


Fig. 12. Force vs distance moved during pull out for glass embedded in low density polyethylene.

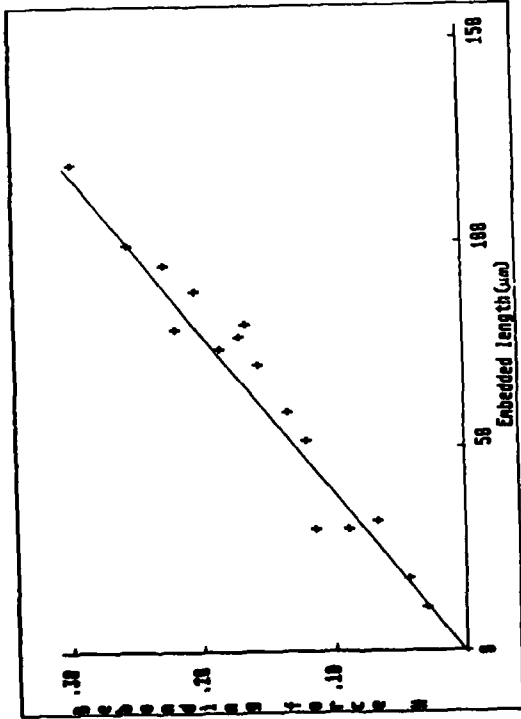


Fig. 9. Debonding force vs embedded length. AS1 fibres in EPON 815 cured at 135°C for 22 h.

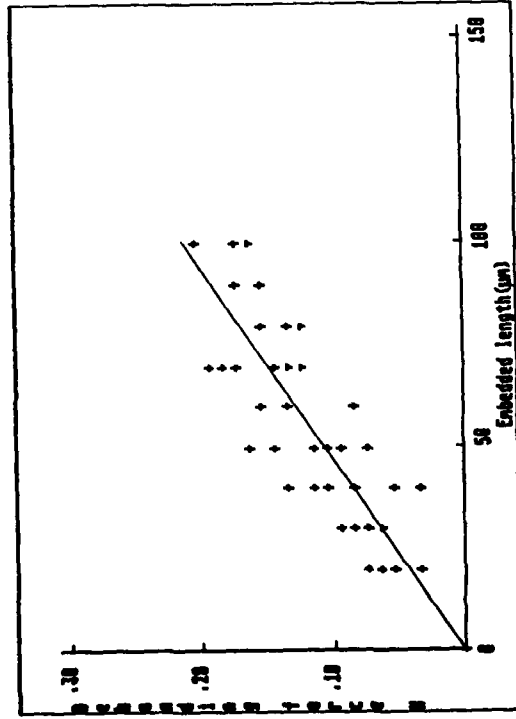


Fig. 10. Debonding force vs embedded length. AS2 fibres in EPON 815 cured at 135°C for 22 h.

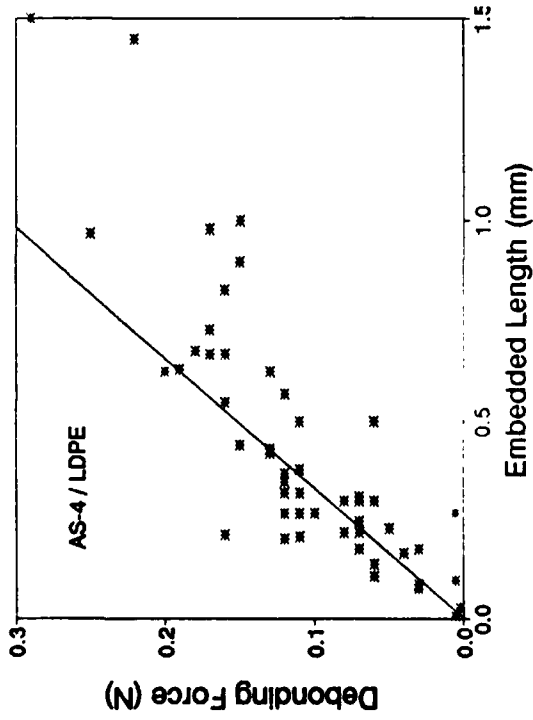


Fig. 13. Debonding force vs embedded length for AS4 fibres in low density polyethylene.

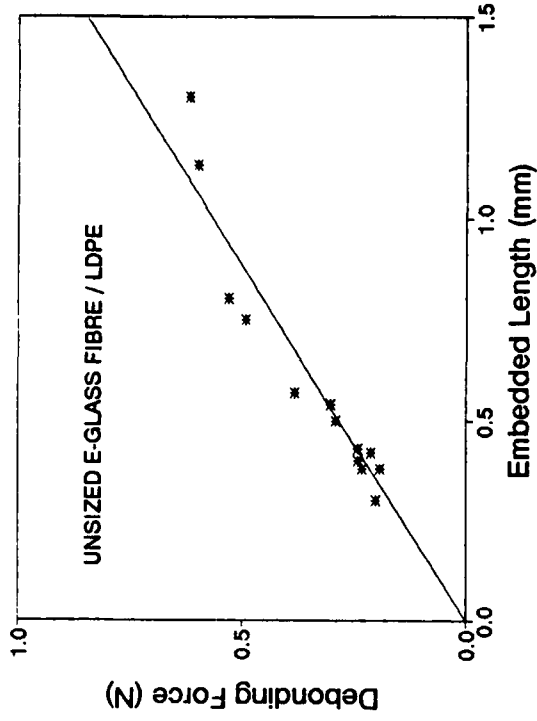


Fig. 15. Debonding force vs embedded length for unsized glass fibres in low density polyethylene.

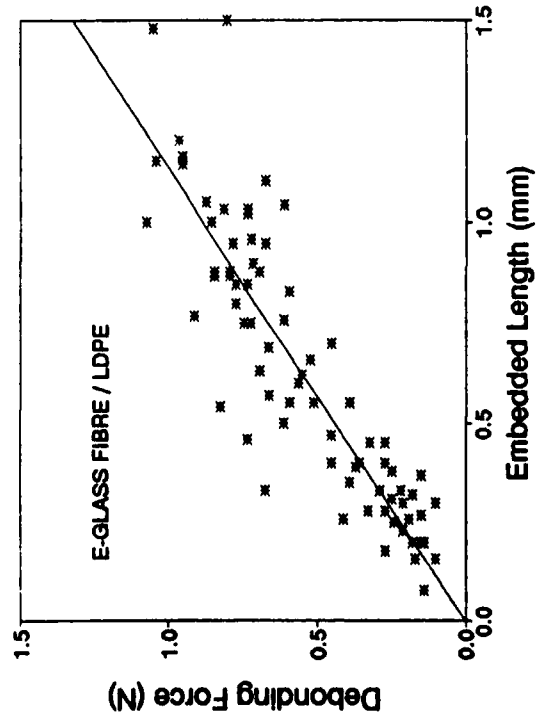


Fig. 14. Debonding force vs embedded length for glass fibres in low density polyethylene.

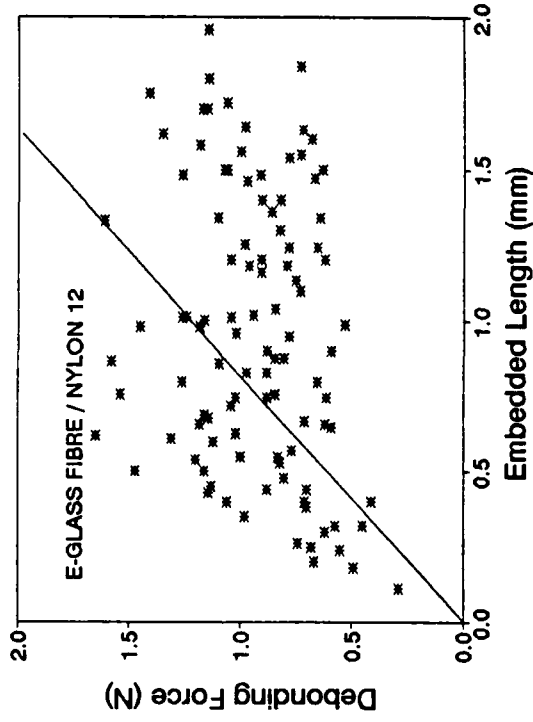


Fig. 16. Debonding force vs embedded length for glass fibres in nylon 12.

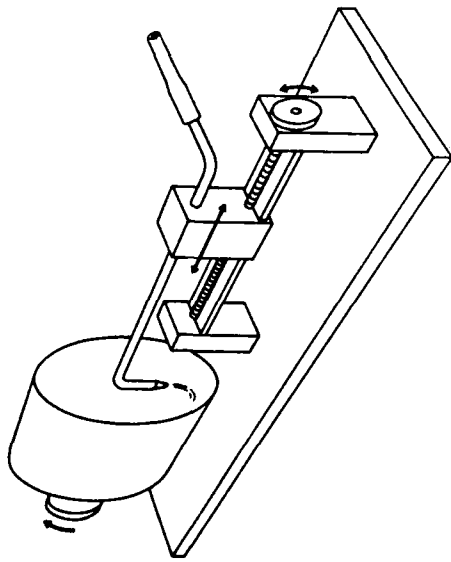


Fig. 17. Schematic drawing of fiber alignment machine.

**Angular distribution of aligned 2 mm fibres**

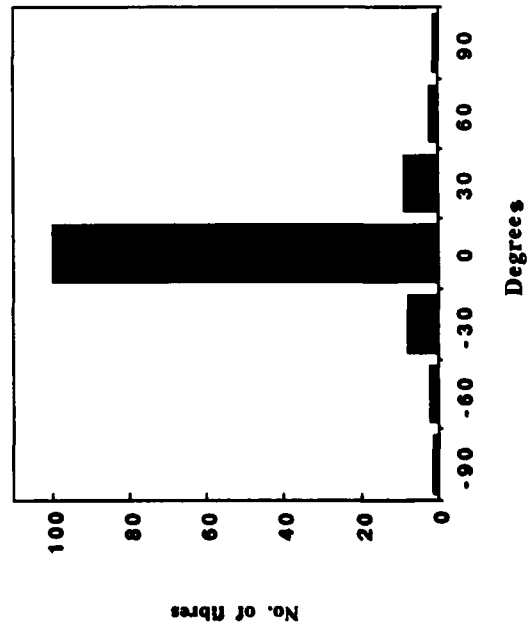


Fig. 18. Angular distributions of 2 mm aligned fibres.

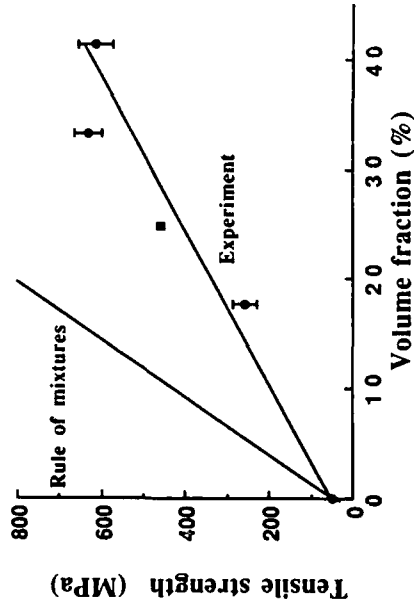


Fig. 19. Tensile strength vs fibre volume fraction for aligned 2 mm carbon fibre composites.

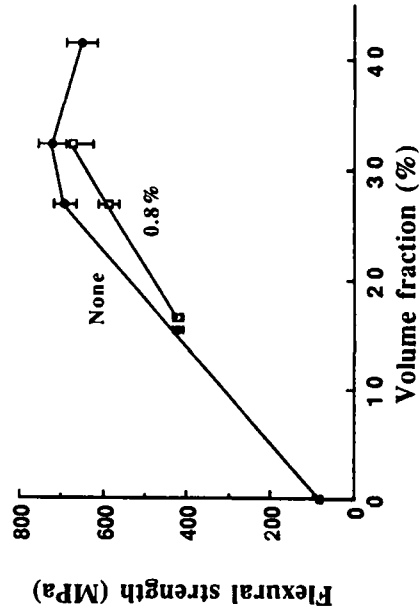


Fig. 20. Flexural strength vs fibre volume fraction for aligned 2 mm carbon fibre composites.

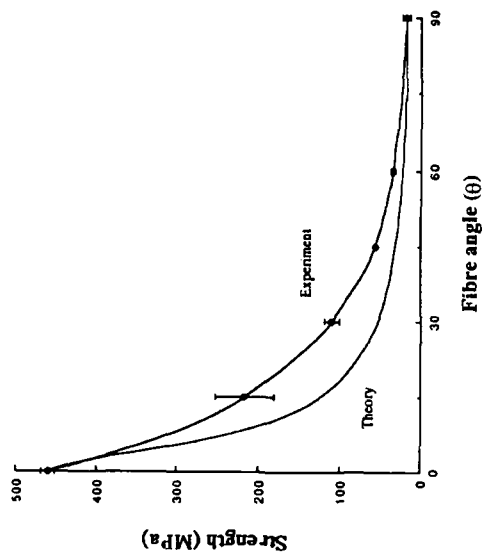


Fig. 23. Off axis strength of 2 mm aligned carbon fibre composites.

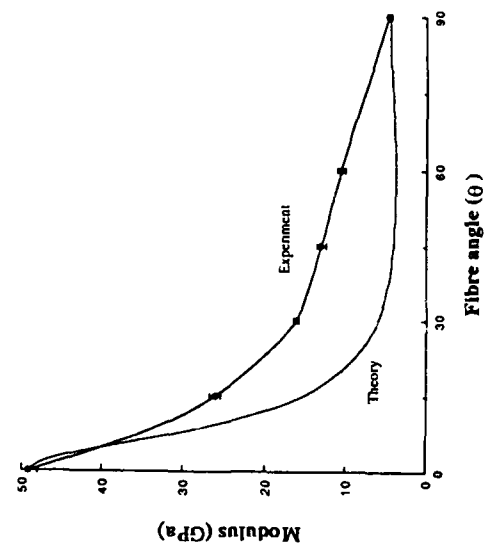


Fig. 24. Off axis Young's modulus of 2 mm aligned carbon fibre composites.

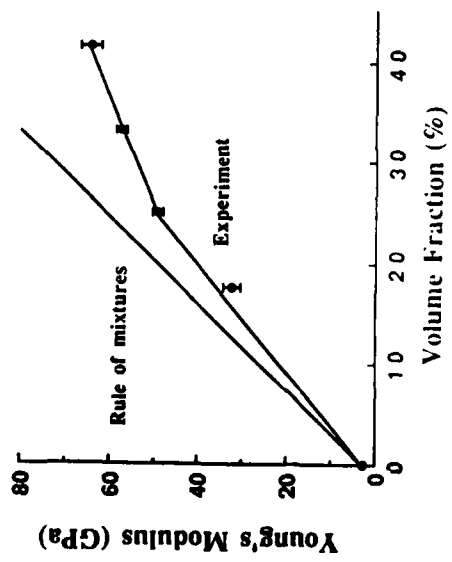


Fig. 21. Young's modulus vs fibre volume fraction for aligned 2 mm carbon fibre composites.

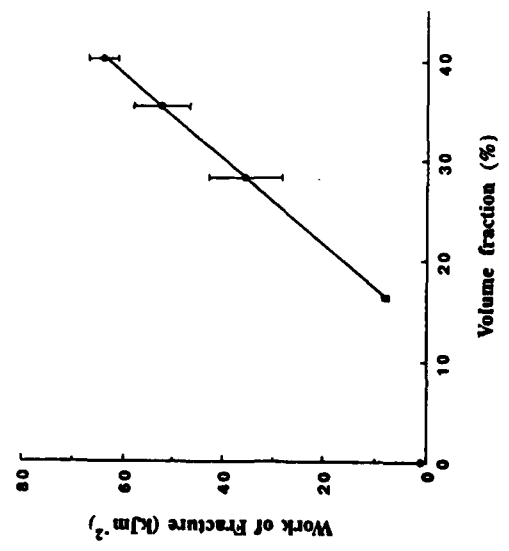


Fig. 22. Work of fracture vs fibre volume fraction for aligned 2 mm carbon fibre composites.